Supporting Information

An Advanced Elastomer with Unprecedented Combination of Excellent Mechanical Properties and High Self-healing Capability

Jie Liu,[§, a,c] Jun Liu,[§, b] Sheng Wang,[a] Jing Huang,[a] Siwu Wu,[a] Zhenghai Tang,[a] Baochun Guo*[,a] and Liqun Zhang*[,b]

FTIR spectra of IR, IR-g-MAn, IR-g-ATA-1:1 and IR-g-ATA

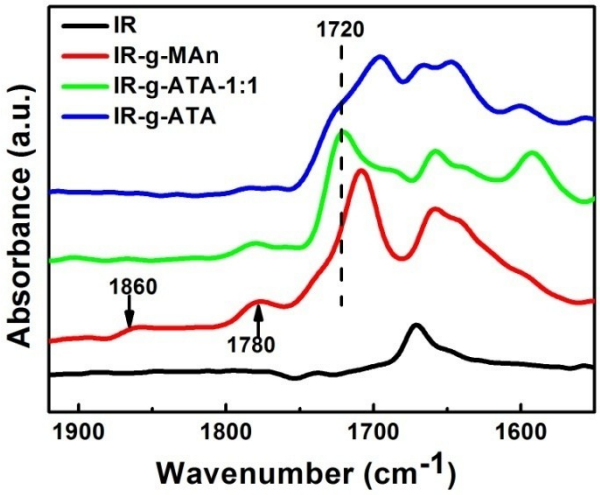

Figure S1 FTIR of IR, IR-g-MAn, IR-g-ATA-1:1 and IR-g-ATA.

FTIR spectra of IR, IR-g-MAn (maleic anhydride grafted IR), IR-g-ATA-1:1 (1:1 ATA/maleic anhydride mole ratio) and IR-g-ATA (2:1 ATA/maleic anhydride mole ratio) are shown in Figure S1. Compared with IR, IR-g-MAn exhibits characteristic peaks of a saturated acid anhydride at 1860 and 1780 cm^{-1}, which are attributed to symmetric and asymmetric C=O stretching, indicating the presence of grafted succinic anhydride on the backbone of IR.[1, 2] After the reaction of ATA with maleic anhydride (IR-g-ATA-1:1), the absorption peaks of anhydride carbonyl groups at 1860 and 1780 cm^{-1} are weakened. Since the ATA/maleic anhydride mole ratio is 1:1 in IR-g-ATA-1:1, carboxylic acid groups are formed (characteristic absorption

peak at 1720 cm-1).[1, 3, 4] When increasing ATA/maleic anhydride mole ratio to 2:1 (Sample IR-g-ATA), most formed carboxylic acid groups will react with ATA, and the peaks of the carboxylic acid groups at 1720 cm^{-1} are greatly weakened, demonstrating that equivalent anhydride group can react with two equivalent ATA. Similar reactions have been also reported by others.[5]

Tensile loading-unloading curves of ZnATA-1/8, ZnATA-2/8 and ZnATA-3/8

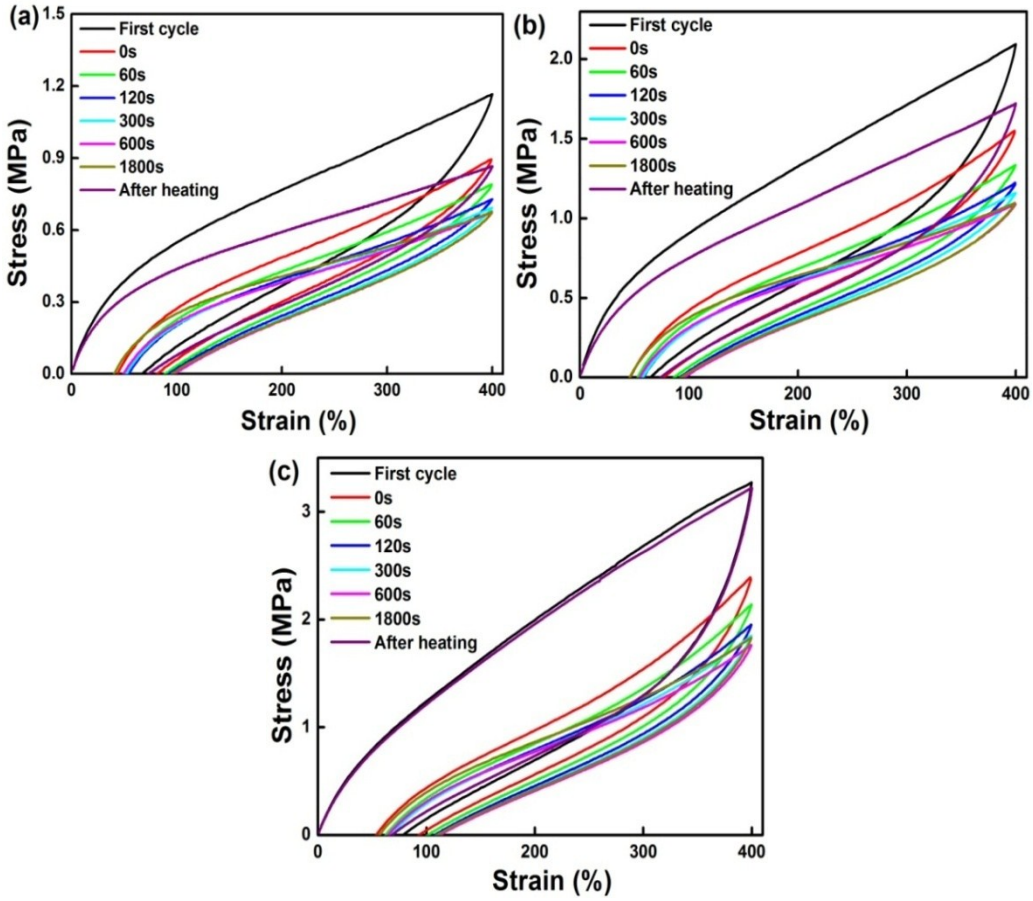

Figure S2 Tensile loading-unloading curves of (a) ZnATA-1/8, (b) ZnATA-2/8 and (c) ZnATA-3/8.

The stress-strain curves of ZnATA-1/8, ZnATA-2/8 and ZnATA-3/8

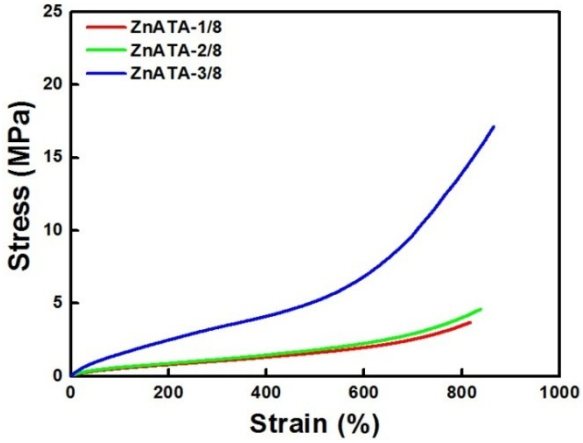

Figure S3 The stress-strain curves of ZnATA-1/8, ZnATA-2/8 and ZnATA-3/8.

XRD Profiles of ZnATA-4/8 at selected strains

In order to confirm the formation of SIC in ZnATA-4/8, XRD profiles at typical strains are depicted in Figure S4. Two diffraction peaks of IR crystal should be recognized near 2ϑ=14° (*200* plane) and 2ϑ=21° (*120* plane) when crystals are formed.[6, 7] As shown in Figure S4, XRD patterns of ZnATA-4/8 at strain of 450% and 600% exhibit a dispersing diffraction peak. When increasing strain to 750%, ZnATA-4/8 shows weak peaks at 2ϑ=14° and 2ϑ=21°. Further increasing strain into 850%, both peaks are intensified. These results demonstrate the formation of SIC at larger strains in ZnATA-4/8.

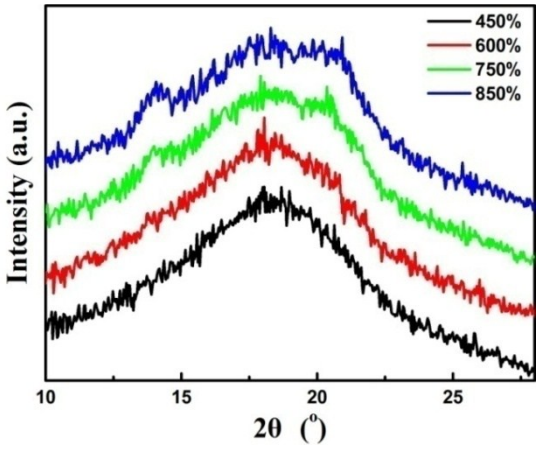

Figure S4 XRD of ZnATA-4/8 at selected strains.

Stress-strain curves of the sample healed at 80 °C

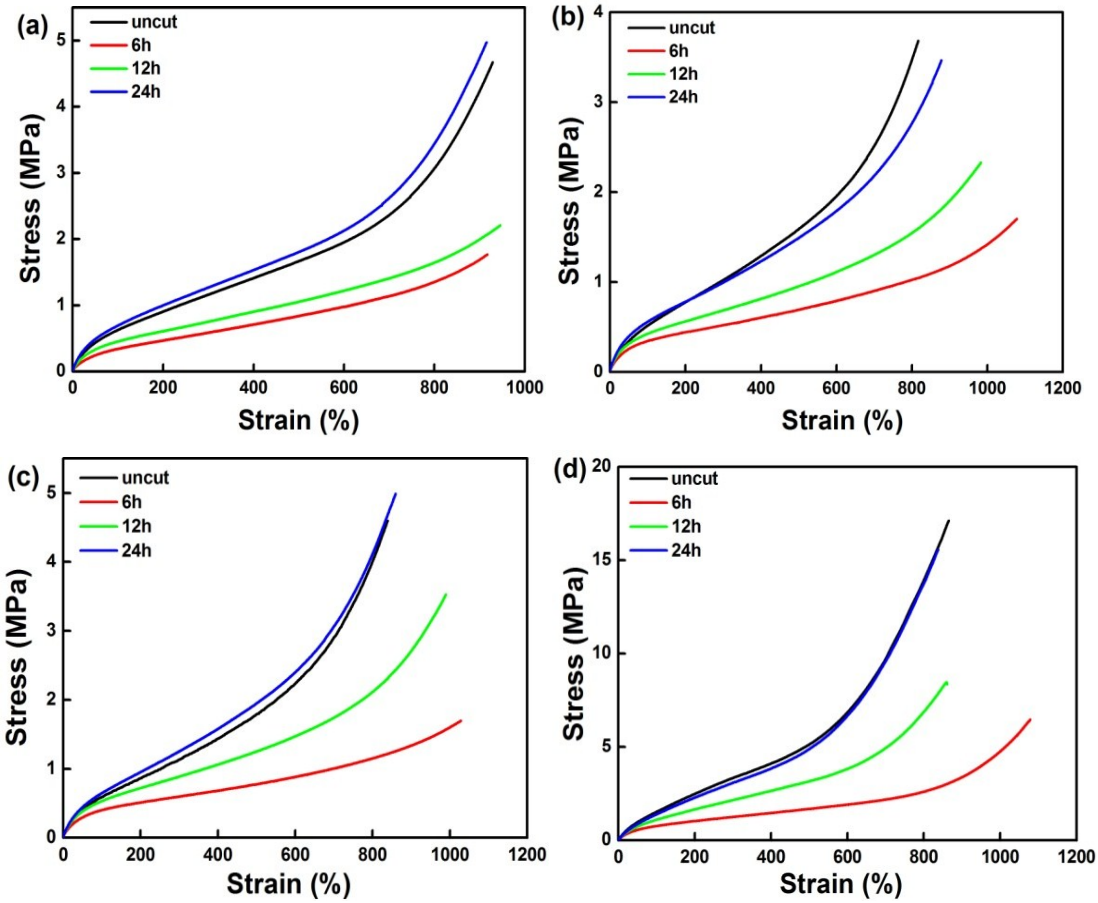

Figure S5 Stress-strain curves of the sample healed at 80 °C for different times. (a)ZnATA-0; (b)ZnATA-1/8; (c) ZnATA-2/8; (d)ZnATA-3/8.

Effects of coordination on the relaxation of the elastomer

The master curves of ZnATA-x were evaluated on the basis of the combined temperature/frequency sweep measurement. A reference temperature (T_0 = -30 °C) was selected, and a horizontal shift factor, α_T, as a function of temperature enabled one to obtain the master curves. The shift factor plots of ZnATA-x are documented in Figure S6. The Williams-Landel-Ferry (WLF) equation (Equation S1) was used to model the time-temperature behavior of ZnATA-x:[8]

$$\log \alpha_T = \frac{-C_1(T - T_0)}{C_2 + (T - T_0)} \qquad (S1)$$

where C_1 and C_2 are the WLF constants and T is the measurement temperature. The values of C_1 and C_2 obtained after fitting the data to the WLF equation are tabulated in Table S2.

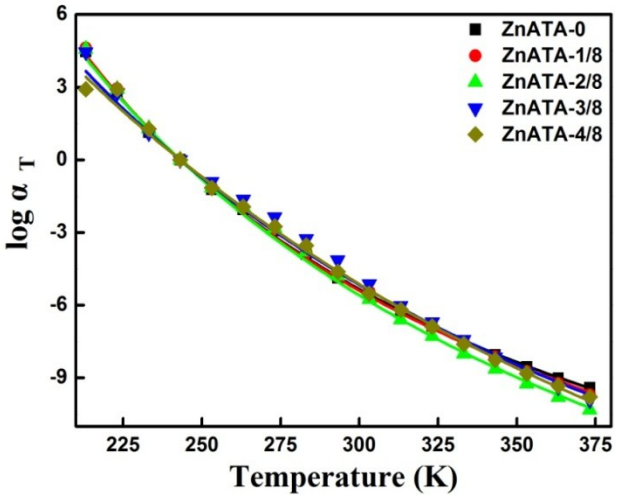

Figure S6 α_T values of ZnATA-x as a function of temperature. The line shown is the best fit WLF equation to the α_T values.

As shown in Figure S7, both G' and G" at higher frequencies do not exhibit much difference after the introduction of the Zn-triazole bonds (comparing ZnATA-x with ZnATA-0). As Zn content increases, the G" relaxation peaks in the low-frequency range shift to lower frequencies (as the black arrow in Figure S7b), indicating the hindrance of rubber viscosity relaxation due to Zn-triazole coordinative complexes.

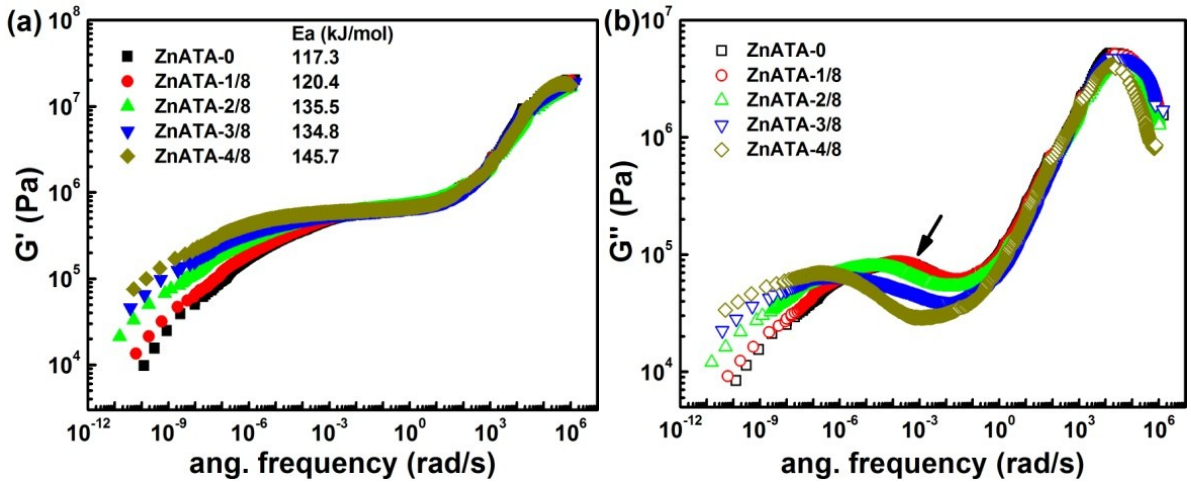

Figure S7 Master curves of the (a) storage modulus and (b) loss modulus based on time-temperature superposition.

To quantitatively evaluate the effect of the Zn-triazole content on the chain mobility, the apparent activation energies (E_a) are determined by substituting the WLF equation into the frequency shift factor in the Arrhenius equation as follows: [8]

$$E_a = R\left(\frac{\mathrm{d}\ln\alpha_T}{\mathrm{d}(1/\mathrm{T})}\right) = 2.303R\left[\frac{C_1C_2\,\mathrm{T}^2}{(C_2+\mathrm{T}-\mathrm{T}_0)^2}\right] \qquad \text{(S2)}$$

The E_a values at 80 °C for each sample are shown in the inset of Figure S7a. The incorporation of Zn-triazole coordination is found to not strongly affect E_a. Compared with ZnATA-0, the increase of E_a in ZnATA-4/8 is less than 25%.

Table S1 The mechanical and healing properties of previously reported materials

Sample	Original Ts（MPa）	Original Elongation (%)	Healing Condition	Healing Effeciengy
Fe- H_2pdca -PDMS[9]	0.23	1800	rt for 48h	90%
Fe-triazole-PDMS[10]	0.5	1600	80 °C for 20h	95.2%
$Zn(OTf)_2$-PDMS[11]	0.63	330	rt for 48h	76%
Co-triazole-PDMS[12]	1.12	560	80 °C for 24h	20.7%
HBN-1% GO[13]	0.5	550	rt for 1h	~100%
SPB-2%[14]	1.8	330	rt for 12h	94%
HN-DGEBA-TGMDA[15]	1.5	325	rt for 24h	~100%
HBP[16]	2	790	rt for 24h	90%
ACON[17]	2	920	50 °C for 3h	83%
Copolymer brush[18]	3	500	rt for 24h	80%
Oligomers with hydrogen bonding[19]	3.5	650	rt for 3h	80%
HDI/PEG400/diol[20]	5.5	180	80 °C for 2.5h	70%
imidazolium-modified BIIR[21]	9	1000	rt for 92h	60%
MD_{50}-F_5[22]	12	450	90 °C for 12h	98%

Note

Ts: Tensile strength; rt: room temperature; PDMS: polydimethylsiloxane; H_2pdca-PDMS: PDMS oligomer that contained 2,6-pyridinedicarboxamide groups; HBN: amine-terminated randomly branched oligomer**;** GO: graphene oxide**;** SPB-2%: the functionalized polybutadiene-COOH and polybutadiene-NH_2 based on ionic hydrogen bonding with 2 wt% of tri-functional thiol as a covalent cross-linker; DGEBA: a bifunctional diglycidyl ether of bisphenol A; TGMDA: a tetrafunctional 4,4'-methylenebis (N,N-diglycidylaniline); HN-50_75%DGEBA_25%TGMDA: hybrid networks containing 75% DGEBA and 25% TGMDA; HBP: a hydrogen-bonding brush polymer consists of a 'hard' polystyrene backbone and 'soft' polyacrylate amide brushes carrying polyvalent hydrogen-bonding sites for dynamic supramolecular assembly; ACON: amide-containing

cyclooctene network; Copolymer brush: copolymer having a glassy polymethylmethacrylate backbone and rubbery polyacrylate-amide brushes**;** HDI/PEG400/diol: alkoxyamine-based diol reacted with tri-functional homopolymer of hexamethylene diisocyanate (tri-HDI) and polyethyleneglycol (PEG); BIIR: bromobutyl rubber; MD_{50}-F_5: Poly-N,N-dimethylacrylamide-co-2-methoxyethyl acrylate+5% Fe_2O_3.

Table S2 Viscoelastic parameters of ZnATA-x

Sample	T_0 (K)	C_1	C_2 (K)
ZnATA-0	243.15	23.31	191.4
ZnATA-1/8	243.15	24.12	197.1
ZnATA-2/8	243.15	28.78	235.8
ZnATA-3/8	243.15	30.77	282.2
ZnATA-4/8	243.15	37.16	354.9

References

1. K. Chino and M. Ashiura, *Macromolecules*, 2001, **34**, 9201-9204.
2. T. Tsujimoto, K. Toshimitsu, H. Uyama, S. Takeno and Y. Nakazawa, *Polymer*, 2014, **55**, 6488-6493.
3. Y. Wang, Q. X. Ai and J. Lu, *J. Polym. Sci., Part A: Polym. Chem.*, 2015, **53**, 1422-1429.
4. J. G. Lim, J. H. Baik, X. Q. Zhang, Y. Son, W. M. Choi and O. O. Park, *Polym. Bull.*, 2002, **48**, 397-405.
5. Aykut A. Ikizler, C. B. Johansson, O. Bekircan, C. Celik., *Acta Poloniae Pharmaceutica-Drug Research*, 1999, **56**,283-288
6. Y. Q. Ren, S. H. Zhao, Q. Yao, Q. Q. Li, X. Y. Zhang and L. Q. Zhang, *Rsc Advances*, 2015, **5**, 11317-11324.
7. G. S. Weng, G. S. Huang, L. L. Qu, Y. J. Nie and J. R. Wu, *J. Phys. Chem. B*, 2010, **114**, 7179-7188.
8. S. Rooj, A. Das, K. W. Stockelhuber, D. Y. Wang, V. Galiatsatos and G. Heinrich, *Soft Matter*, 2013, **9**, 3798-3808.
9. C. H. Li, C. Wang, C. Keplinger, J. L. Zuo, L. Jin, Y. Sun, P. Zheng, Y. Cao, F. Lissel, C. Linder, X. Z. You and Z. A. Bao, *Nat. Chem.*, 2016, **8**, 619-625.
10. X. Y. Jia, J. F. Mei, J. C. Lai, C. H. Li and X. Z. You, *Macromol. Rapid Comm.*, 2016, **37**, 952-956.
11. Y. L. Rao, A. Chortos, R. Pfattner, F. Lissel, Y. C. Chiu, V. Feig, J. Xu, T. Kurosawa, X. D. Gu, C. Wang, M. Q. He, J. W. Chung and Z. N. Bao, *J. Am. Chem. Soc.*, 2016, **138**, 6020-6027.
12. X. Y. Jia, J. F. Mei, J. C. Lai, C. H. Li and X. Z. You, *Chem. Commun.*, 2015, **51**, 8928-8930.
13. C. Wang, N. Liu, R. Allen, J. B. H. Tok, Y. P. Wu, F. Zhang, Y. S. Chen and Z. N. Bao, *Adv. Mater.*, 2013, **25**, 5785-5790.
14. D. Wang, J. Guo, H. Zhang, B. C. Cheng, H. Shen, N. Zhao and J. Xu, *J. Mater. Chem. A*, 2015, **3**, 12864-12872.
15. F. Sordo, S. J. Mougnier, N. Loureiro, F. Tournilhac and V. Michaud, *Macromolecules*, 2015, **48**, 4394-4402.
16. Y. L. Chen, A. M. Kushner, G. A. Williams and Z. B. Guan, *Nat. Chem.*, 2012, **4**, 467-472.
17. J. A. Neal, D. Mozhdehi and Z. B. Guan, *J. Am. Chem. Soc.*, 2015, **137**, 4846-4850.
18. Y. L. Chen and Z. B. Guan, *Polymer*, 2015, **69**, 249-254.
19. P. Cordier, F. Tournilhac, C. Soulie-Ziakovic and L. Leibler, *Nature*, 2008, **451**, 977-980.

20. C. E. Yuan, M. Z. Rong and M. Q. Zhang, *Polymer*, 2014, **55**, 1782-1791.
21. A. Das, A. Sallat, F. Bohme, M. Suckow, D. Basu, S. Wiessner, K. W. Stockelhuber, B. Voit and G. Heinrich, *Acs Appl. Mater. Inter.*, 2015, **7**, 20623-20630.
22. X. Q. Feng, G. Z. Zhang, Q. M. Bai, H. Y. Jiang, B. Xu and H. J. Li, *Macromol. Mater. Eng.*, 2016, **301**, 125-132.